

Tables and figures to accompany

Landslides, earthquakes, and sedimentation rate in passive and active margins

By ten Brink, U.S., Andrews, B.D., and Miller, N.C.

Contents

Tables

Table DR1 – Bathymetry data sources

Table DR2- Morphological parameters, earthquake recurrence, and sedimentation rate for the ten margins

Table DR3 – Data sources for the earthquake recurrence and sedimentation rates used in Table DR2.

Figures

Fig. DR1a,b - Bathymetry maps of individual margins. Color denotes depth with depth ranges given in Table DR2. Total area of the polygon(s) in each margin is listed in Table DR2. Mapped scar areas are in black. Data sources are given in Table DR1. Dashed white lines are the locations of the depth profiles shown in c). c – Depth profiles across the margins to facilitate comparison between the general shape of the different margins.

Fig. DR2a,b,c - Similar figures to Figures 2a,b,c, but excluding scars and margin areas with gradients < 3°.

2016187_Polygon Data.zip

MarginBounds.kmz shows the polygons of all the margin areas shown in Fig. DR1 as black lines surrounded by white lines.

ScarBounds.kmz shows the polygons of all the landslide scars marked in black in Fig. DR1.

Table DR1

Table DR1 – Bathymetry data sources

Margin name	Multibeam bathymetry surveys	Resolution (m)*	Source
Cascadia N. (Washington)	TN265, AVON09MV, MGL1212	50	NOAA-National Centers for Environmental Information
Cascadia N. (Oregon)	Compilation of various surveys	100	NOAA- National Centers for Environmental Information* (http://efh-catalog.coas.oregonstate.edu/bathy/)
Cascadia S. (Oregon)	Compilation of various surveys	100	NOAA- National Centers for Environmental Information* (http://efh-catalog.coas.oregonstate.edu/bathy/)
Guatemala-El Salvador	SO173_L2	100	Federal Maritime and Hydrographic Agency of Germany
Israel	Sade et al., 2007	50	Gadol, 2015**
Makran	SO123	100	Federal Maritime and Hydrographic Agency of Germany
Muertos Trough	Compilation of various sources	50	Andrews et al., 2014 (http://pubs.usgs.gov/of/2013/1125/pdf/ofr2013-1125.pdf)
Queen Charlotte Fault	CCGS Vector (Barrie et al., 2013_	10	Canadian Hydrographic Service and Canadian Geological Survey**
Nicaragua-Costa Rica	SO163_L1 &L2, SO144, SO144_L3	100	Federal Maritime and Hydrographic Agency of Germany
Nicaragua-Costa Rica	EW0005, EW0104	100	NOAA- National Centers for Environmental Information
N. Sumatra Trench	HMS Scott (Henstock et al., 2006)	50	National Oceanographic Centre, Southampton, U.K.
U.S. Atlantic Margin	Compilation of various sources	50	Andrews et al., 2013 (http://pubs.usgs.gov/of/2012/1266/appendix_1.html)

Comments:

*The vertical accuracy of the data is $\leq 0.2\%$ of the water depth for a 12 kHz sonar (de Moustier, 2001), the lowest frequency sonar used in this study. It is difficult, however, to quantify the true vertical resolution of the data. A scarp is evident as an abrupt change in slope between pixels. Scarp identification therefore depends on the gradient of the surrounding pixels, the grid size, and the lateral continuity of the scarp.

**All bathymetry data, with the exception of data sources marked by *, were reprocessed using Caris Hips 9.0 from raw line files and the vessel configuration files, cleaned and gridded, following the procedure outlined in Andrews et al., 2013. We used already gridded data sets from Israel (50 m), Queen Charlotte fault (5 m), and Oregon (100 m) because of lack of access to the raw data.

References cited:

- Andrews, B. D., Chaytor, J. D., ten Brink, U. S., Brothers, D. S., and Gardner, J. V., 2013, Bathymetric terrain model of the Atlantic Margin for marine geological investigations: U.S. Geological Survey Open-File Report no. 2012-1266.
- Andrews, B. D., Uri, S., Danforth, W. W., Chaytor, J. D., Bruña, J.-L. G., Estrada, P. L., and Carbó-Gorosabel, A., 2014, Bathymetric terrain model of the Puerto Rico Trench and the northeastern Caribbean region for marine geological investigations: US Geological Survey Open-File Report no. 2331-1258.
- Barrie, J. V., Conway, K. W., and Harris, P. T., 2013, The Queen Charlotte fault, British Columbia: Seafloor anatomy of a transform fault and its influence on sediment processes: Geo-Marine Letters, v. 33, no. 4, p. 311-318.
- De Moustier, C., Field evaluation of sounding accuracy in deep water multibeam swath bathymetry, in Proceedings OCEANS, 2001, V. 3, IEEE, p. 1761-1765.
- Henstock, T. J., McNeill, L. C., and Tappin, D. R., 2006, Seafloor morphology of the Sumatran subduction zone: Surface rupture during megathrust earthquakes?: Geology, v. 34, no. 6, p. 485-488.
- Gadol, O., 2015, Submarine slides: shaping of the continental slope offshore Israel, M.Sc. thesis, University of Haifa, 99 pp.
- Sade, A.R., Hall, J.K., Amit, G., Golan, A., Gur-Arieh, L., Tibor, G., 2007, The Israel national bathymetric survey - a new look at the seafloor off Israel. Israel Journal of Earth Sciences, v. 55, p. 185–187.

Table DR2**Table DR2- Morphological parameters, earthquake recurrence, and sedimentation rate for the regions bounded by polygons in Fig. DR1**

Margin name	Range of water depths (m)*	Margin area (km ²)	Total failure area (km ²)	Total failure volume (km ³)	Mean slide thickness (m)**	Mean margin gradient (°)	% margin > 3°	% scar area > 3°	Scar fraction	Scar fraction >3° ***	Mean slide gradient (°)****	Earthquake recurrence (yr)	Sedimentation rate (cm/ kyr)	Inter-seismic sediment thickness (cm)
Cascadia N	668 - 2322	24171	579	31.56	63	5.4±5.9	54.8	85.2	0.02	0.04	6.9	500±75	9.8±1.3	4.9±1.4
Cascadia S	104 - 3111	12407	1638	109.91	78	5.7±5.3	61.3	87.9	0.13	0.19	8.8	500±75	9.8±1.3	4.9±1.4
Guatemala ElSalvador	174 - 6645	31076	560	42.06	78	6.9±4.2	86.0	90.6	0.02	0.02	6.6	60±15	8.5±4.5	0.5±0.4
Israel [†]	83 - 1130	2256	615	8.92	14	2.6±2.1	31.2	45.1	0.30	0.39		2604±1302	66.0±42.0	171.9±196.0
Makran	1226-3369	8675	424	20.05	54	6.0±6.3	52.5	85.9	0.05	0.08	7.2	175±74	70.5±23.3	12.3±9.3
Muertos	297 - 5579	37191	2065	118.15	63	6.1±5.2	69.0	79.0	0.06	0.06	5.6	1855±1232	4.3±2.1	8.0±9.2
Nicaragua	306 - 5797	14133	546	55.11	108	6.4±3.9	85.0	95.4	0.04	0.04	8.2	75±19	35.0±21.0	2.6±2.2
Queen Charlotte F	7 - 1944	2861	25	0.53	24	8.2±9.2	80.0	97.2	0.01	0.01	12.8	100±30	1.0±0.5	0.1±0.1
N. Sumatra	393 - 4969	19067	1142	61.27	63	12.3±9.1	82.5	96.1	0.06	0.07	14.3	150±50	155.0±25.0	23.3±11.5
U.S. Atlantic	463 - 1962	4538	2407	55.91 [^]	56 ^{^^}	2.8±1.5	50.7	54.6	0.53	0.57		15000±5000	13.6±6 ^{^^^} 72.5±7.5 ^{^^^^}	203.25±157 1087.5±507.9

Comments:

Average values and uncertainties in columns 12 and 13 are calculated from the range of values listed in Table DR3.

[&]Landslide scars in the Israeli margin were mapped and measured by Gadol (2015).

*Range of water depths includes the slope from the shelf-edge break to the trench axis (in convergent margins) and the rise in non-convergent margins. Bathymetry is unavailable from the uppermost slope of the Makran margin and the wide terrace at the base of the Queen Charlotte Fault margin.

**Mean slide thickness is the total slide volume divided by the total slide area.

***Calculated by dividing that part of the margin area covered by scars with a gradient >3° by the part of the margin area with a gradient >3°.

****Mean slide gradient is the sea floor gradient prior to failure, weighted to slide area. Sea floor gradient prior to failure is calculated by fitting a smooth surface that connects the tops of the slide scarp (see ten Brink et al., 2006; Chaytor et al., 2009 for more details).

[†]Approximate estimate because of the difficulty of associating scarps with individual scars.

[^]Based on total area and volume for the entire U.S. Atlantic margin from Chaytor et al. (2009).

^{^^}Sedimentation rate for the Holocene.

^{^^^}Sedimentation rate for the Pleistocene.

References cited:

- Chaytor, J. D., ten Brink, U. S., Solow, A. R., and Andrews, B. D., 2009, Size distribution of submarine landslides along the US Atlantic margin: *Marine Geology*, v. 264, p. 16-27.
- Gadol, O., 2015, Submarine slides: shaping of the continental slope offshore Israel, M.Sc. thesis, University of Haifa, 99 pp.
- ten Brink, U. S., Geist, E. L., and Andrews, B. D., 2006, Size distribution of submarine landslides and its implication to tsunami probability in Puerto Rico: *Geophys. Res. Lett.*, v. 33, L11307, doi:10.1029/2006GL026125.

Table DR3

TABLE DR3- DATA SOURCES FOR SEDIMENTATION RATE AND EARTHQUAKE RECURRENCE INTERVAL

Margin Name	Sedimentation Rate	Earthquake Recurrence Interval
Cascadia	8.5-11 cm/kyr ¹	500-600 yr ¹²
Guatemala – El Salvador	DSDP leg 84: hole 570; 13 cm/kyr ² (Pleistocene); hole 567 (within a canyon) – 4 cm/kyr ² (Pleistocene)	M7 – 41-50 yr ¹³ ; M7.5 – 40 yr ¹³ ; Northern Nicaragua and El Salvador west of 87°W ¹² : 63-91 yr; Guatemala 66-91 ¹²
Israel	Northern part: 24.7 cm/kyr (last 14.8 kyr) ³ ; 29.4 cm/kyr (last 8.8 kyr) ³ . Southern part: 24.1 (last 11.6 kyr) ⁴ ; 108 cm/kyr (last 3.7 kyr) ⁵	Recurrence is based on the following b-values: Log (N/yr) = 0.97*M+3.67 (Dead Sea Basin) and Log(N/yr) = 0.85M+2.36 (Northern Jordan Valley) ¹⁴ . M7 every 1318 yr and 3890 yr, respectively.
Muertos Trough	Core 8: 2.2 cm/kyr (last 11,810 yr) ⁶ ; Core 9: 6.4 cm/kyr (last 10,610 yr) ⁶ ; Core 9: 5.11 cm/kyr (last 30,500 yr) ⁶	Maximum displacement for reverse faults log (max. displ.) = -1.84+.29M ¹⁵ yields 1.55 m for M7 and 2.16 for M7.5. Assuming 50% coupling, the average displacement per earthquake is expected to be 3.1 m - 4.32 m. Estimated convergence rate across Muertos Trough is 1-3 mm/yr ¹⁶ . Hence estimate recurrence interval is: 1855±1232.
Makran	Cores NIOP470 and NIOP471 ⁷ are located within the multibeam bathymetry grid. An age of 8 kyr was identified and marked in these cores ⁷ by correlation with other dated cores outside the multibeam bathymetry grid. Measured graphically, the marked age is at 68% and 80% of the core length (550 cm and 940 cm respectively), yielding average sedimentation rates of 47 cm/kyr and 94 cm/kyr, respectively.	100-250 yr ⁷ ; 175 yr or longer ²¹
Nicaragua – northern Costa Rica	30-40 cm/kyr ⁸ (Holocene and latest Pleistocene) but with large variations. In detail: Hole M54 - 2 35 cm/kyr (between 15-25 kyr BP), and 13.3 cm/kyr (more recent); Hole M54-3 – 2.2 cm/kyr;	M7 – 53-68 yr ¹³ ; M7.5 – 51-99 yr ¹³ ; Northern Nicaragua –El Salvador west of 87°W: 63-91 yr ¹²

SO173-18 - 90 cm/ky; M66-178 (last 17 kyr) - 16.52 cm/kyr; SO173-11 - 50 cm/kyr

Queen Charlotte Fault	~0 to 40,000 ^{14}C yr BP in 3 cores within the fault valley ⁹ (Vaughn Barrie, written. Comm., 8/24/2015)	70-130 yr ¹² ; 69 yr ¹³ ; 713 yr for thrust faults but ¼-1/5 of that for strike-slip earthquakes ¹⁷
N. Sumatra	Holocene: 180 cm/kyr ¹ , also 130-170 cm/kyr ¹	Farther south off Central Sumatra: Super cycles every ~200 yr, 6-8 events caused relative sea level change in the past 700 yr ¹⁸ (700/6=118 yr). Northern Sumatra – M7.6 in 1907, M7.2 in 2002, M9.1 in 2004, M7.3 in 2008 ¹⁹
U.S. Atlantic margin (Southern New England)	Holocene sedimentation rates ¹⁰ : Core 463-2PC 10.8 cm/kyr; 463-15PC - 7.6 cm/kyr; Core 463-16PC – 17 cm/kyr; Core 463-18PC – 9.3 cm/kyr; Core 463-19PC – 19.73 cm/kyr; Core 463-21PC – 11.23 cm/kyr Pleistocene sedimentation rate: Site 1073 (in open slope 60 km south of mapped polygon) >65 cm/ky up to ~80 cm/ky ¹¹ ;	Landslides are dated at 10,000-20,000 ²⁰ . If they were generated by earthquakes, then the last earthquake occurred 15,000±5000 yr ago.

¹Sumner, E. J., Siti, M. I., McNeill, L. C., Talling, P. J., Henstock, T. J., Wynn, R. B., Djajadihardja, Y. S., and Permana, H., 2013, Can turbidites be used to reconstruct a paleoearthquake record for the central Sumatran margin?: Geology, v. 41, p. 763-766, Data repository and references therein.

²Shipboard Scientific Party, 7. Site 570.; Baltuck M., R. von Huene, and R.J. Arnott, 43. Sedimentology of the Western Continental Slope of Central America, in von Huene R., Auboin, J., et al. (eds.), Initial Reports DSDP leg 84 Washington, D.C.

³Hammann, Y., Ehrmann, W., Schmiedl, G., Krüger, S., Stuut, J.-B., and Kuhnt, T., 2008, Sedimentation processes in the Eastern Mediterranean Sea during the Late Glacial and Holocene revealed by end-member modelling of the terrigenous fraction in marine sediments: Marine Geology, v. 248, p. 97-114.

⁴Castaneda I. S., Schefuß, E., Pätzold, J., Sinninghe Damsté, J. S., Weldeab, S., and Schouten, S., 2010, Millennial-scale sea surface temperature changes in the eastern Mediterranean (Nile River Delta region) over the last 27,000 years: Paleoceanography, v. 25, PA1208, doi:10.1029/2009PA001740.

⁵Schilman B., Bar-Matthews, M., Almogi-Labin, A., and Luz, B., 2001, Global climate instability reflected by Eastern Mediterranean marine records during the late Holocene: Palaeogeography, Palaeoclimatology, Palaeoecology, v. 176, p. 157-176.

⁶Hoy S. K., Chaytor, J. D., and ten Brink, U.S., 2014, Core data from offshore Puerto Rico and the US Virgin Islands: US Geological Survey Open-File Report no. 2331-1258.

⁷Bourget J., Zaragoza, S., Ellouz-Zimmermann, S., Ducassou, E., Prins, M., Garlan, T., Lanfumey, V., Schneider, J.-L., Rouillard, P., and Giraudeau, J., 2010, Highstand vs. lowstand turbidite system growth in the Makran active margin: Imprints of high-frequency external controls on sediment delivery mechanisms to deep water systems: Marine Geology, v. 274, p. 187-208.

- ⁸Kutterolf , S., Freundt, A., and Perez, W., 2008, Pacific offshore record of plinian arc volcanism in Central America: 2. Tephra volumes and erupted masses: *Geochemistry, Geophysics, Geosystems*, v. 9, Q02S03, doi:10.1029/2007GC001826.
- ⁹Barrie, J. V., Conway, K. W., and Harris, P. T., 2013, The Queen Charlotte fault, British Columbia: Seafloor anatomy of a transform fault and its influence on sediment processes: *Geo-Marine Letters*, v. 33, p. 311-318.
- ¹⁰Chaytor, J. D., ten Brink, U. S., Baxter, C. D. P., Brothers, D. S., and Hallam, T. D., 2015, Morphology and Age of the Southern New England Landslide Zone: AGU Fall Meeting abstract.
- ¹¹Austin, J. A., Jr., Christie-Blick, N., Malone, M. J., et al. 1998, Proceedings of the Ocean Drilling Program, Initial Reports, Vol. 174A Ch. 5, Site 1073A.
- ¹²Nishenko, S. P., 1991, Circum-Pacific seismic potential: 1989–1999, *PAGEOPH*, v. 135, p. 169-259.
- ¹³Goes S. D., 1996, Irregular recurrence of large earthquakes: an analysis of historic and paleoseismic catalogs: *Journal of Geophysical Research*, v. 101, p. 5739-5749.
- ¹⁴Hamiel, Y., Amit, R., Begin, Z., Marco, S., Katz, O., Salamon, A., Zilberman, E., and Porat, N., 2009, The seismicity along the Dead Sea Fault during the last 60,000 years: *Bulletin of the Seismological Society of America*, v. 99, p. 2020-2026.
- ¹⁵Wells, D. L., and Coppersmith, K. J., 1994, New empirical relationships among magnitude, rupture length, rupture width, rupture area, and surface displacement: *Bulletin of the Seismological Society of America*, v. 84, p. 974-1002.
- ¹⁶Benford, B., DeMets, C., and Calais, E., 2012, GPS estimates of microplate motions, northern Caribbean: evidence for a Hispaniola microplate and implications for earthquake hazard: *Geophysical Journal International*, v. 191, p. 481-490.
- ¹⁷Lay, T., Ye, L., Kanamori, H., Yamazaki, Y., Cheung, K. F., Kwong, K., and Koper, K. D., 2013, The October 28, 2012 M w 7.8 Haida Gwaii underthrusting earthquake and tsunami: Slip partitioning along the Queen Charlotte fault transpressional plate boundary: *Earth and Planetary Science Letters*, v. 375, p. 57-70.
- ¹⁸Sieh K., Natawidjaja, D. H., Meltzner, A. J., Shen, C.-C., Cheng, H., Li, K.-S., Suwargadi, B. W., Galetzka, J., Philibosian, B., and Edwards, R. L., 2008, Earthquake supercycles inferred from sea-level changes recorded in the corals of west Sumatra: *Science*, v. 322, p. 1674-1678.
- ¹⁹Kanamori H., Rivera, L., and Lee, W. H., 2010, Historical seismograms for unravelling a mysterious earthquake: The 1907 Sumatra Earthquake: *Geophysical Journal International*, v. 183, p. 358-374.
- ²⁰ten Brink, U. S., Chaytor, J. D., Geist, E. L., Brothers, D. S., and Andrews, B. D., 2014, Assessment of tsunami hazard to the US Atlantic margin: *Marine Geology*, v. 353, p. 31-54.
- ²¹Byrne, D. E., L.R. Sykes, and D.M. Davis, 1992, Great thrust earthquakes and aseismic slip along the plate boundary of the Makran subduction zone, *Journal of Geophysical Research*, v. 97, p. 449–478.

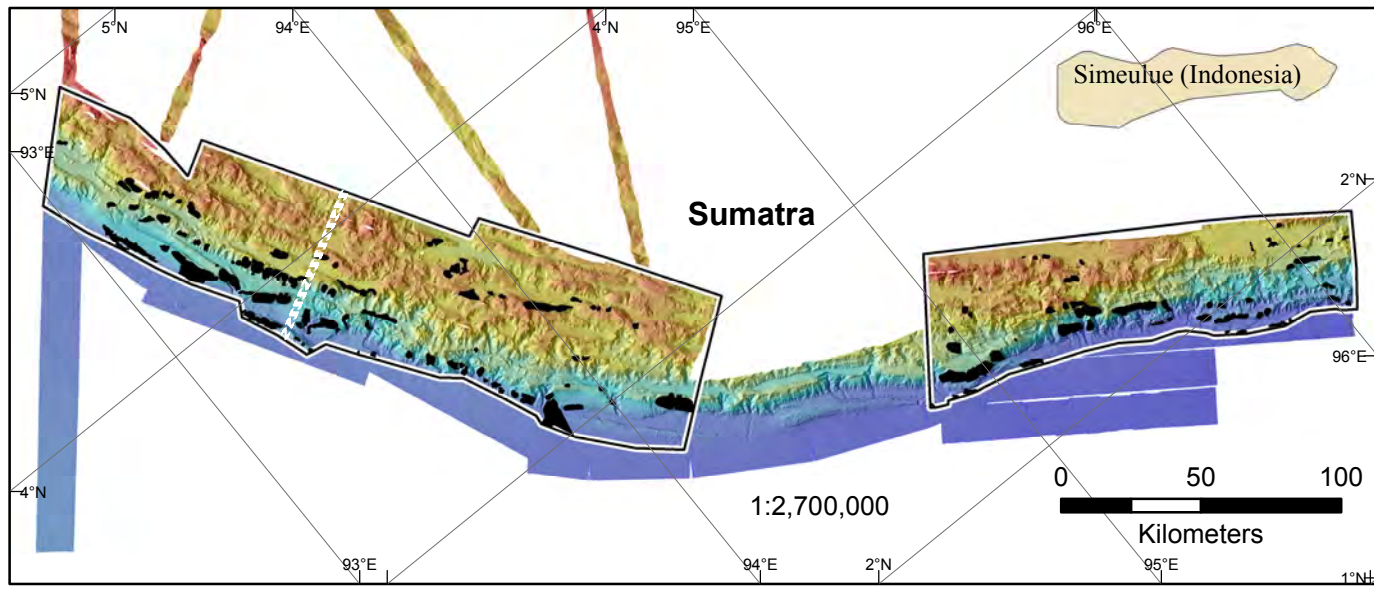
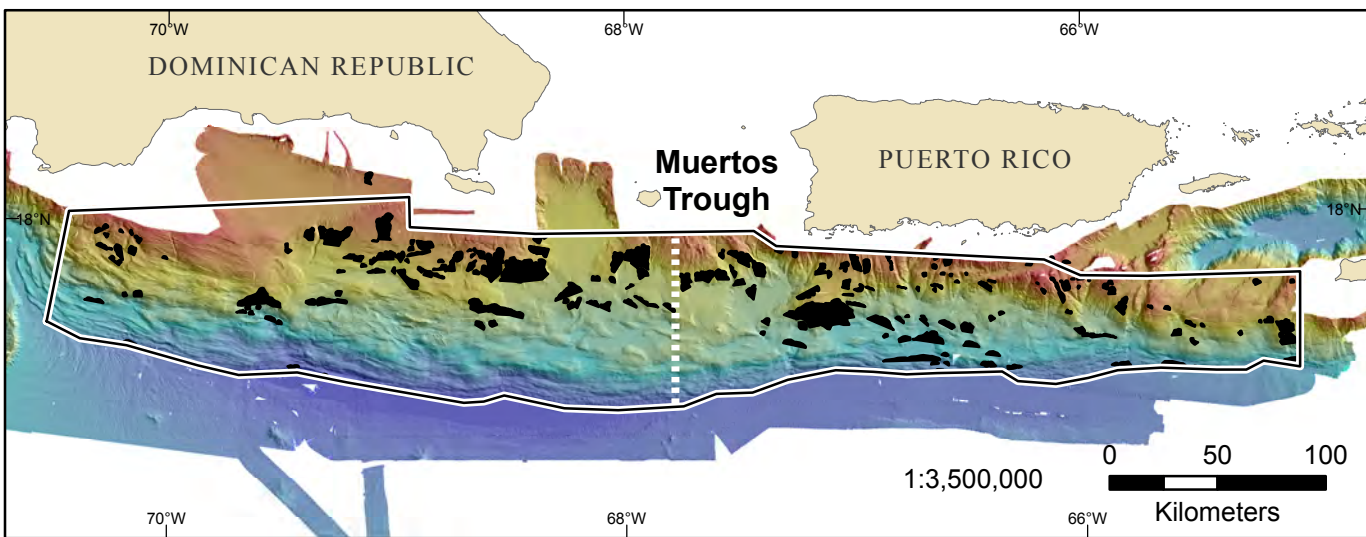
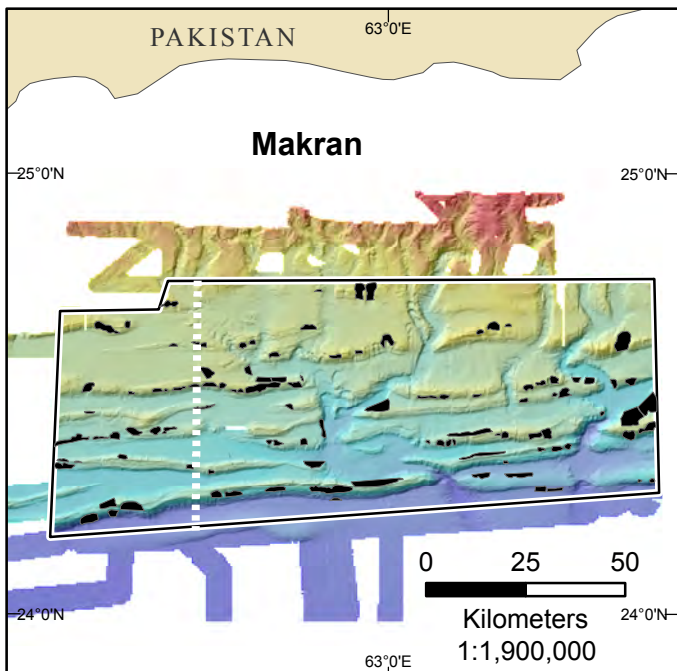
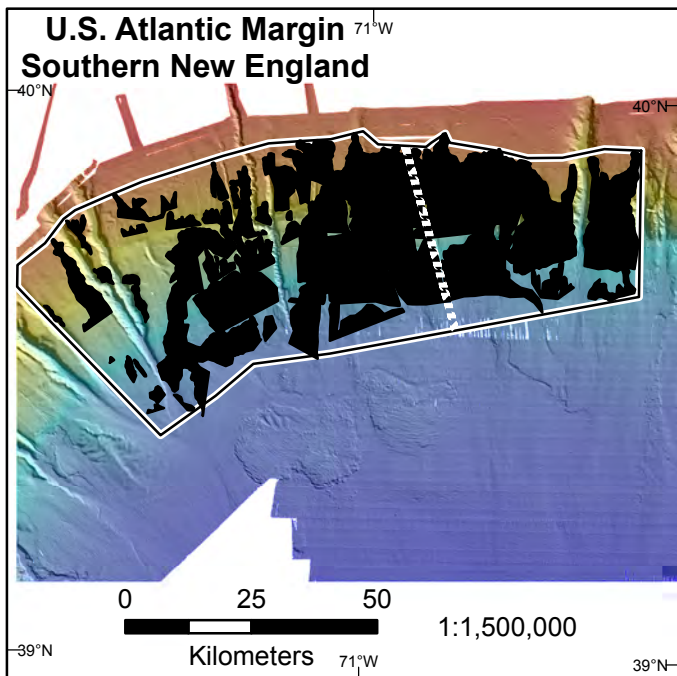


Figure DR1a

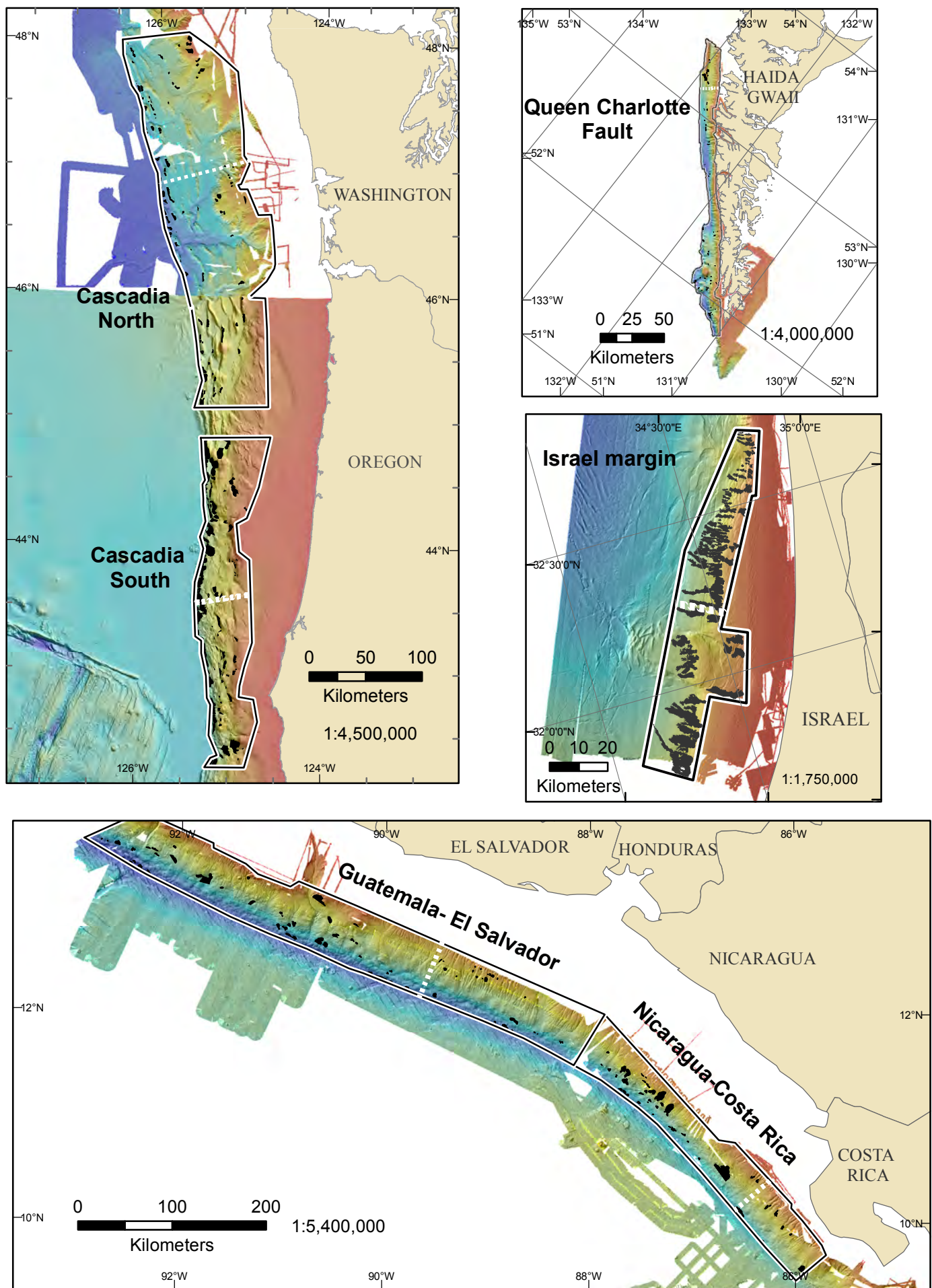


Figure DR1b

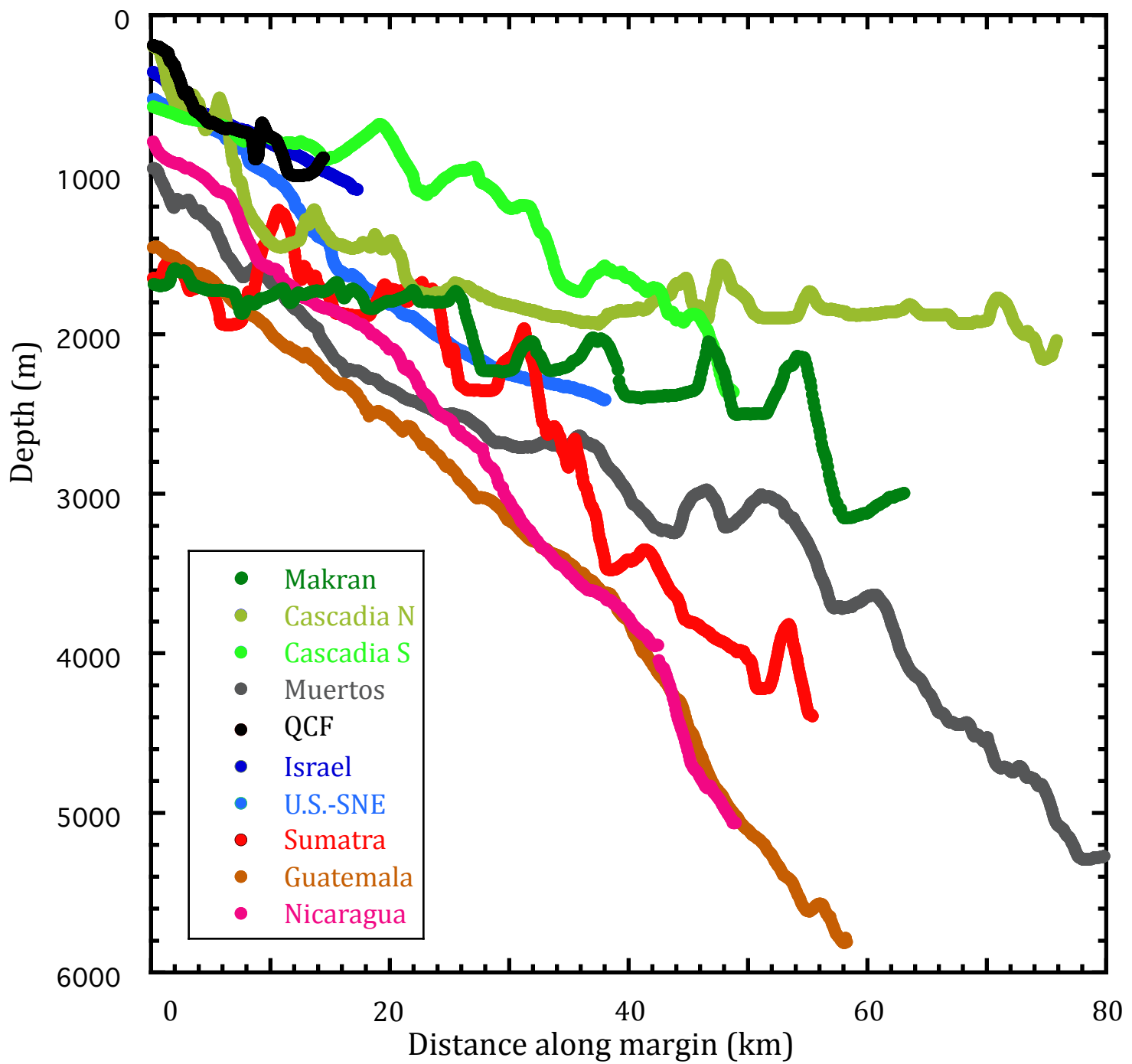


Figure DR1c

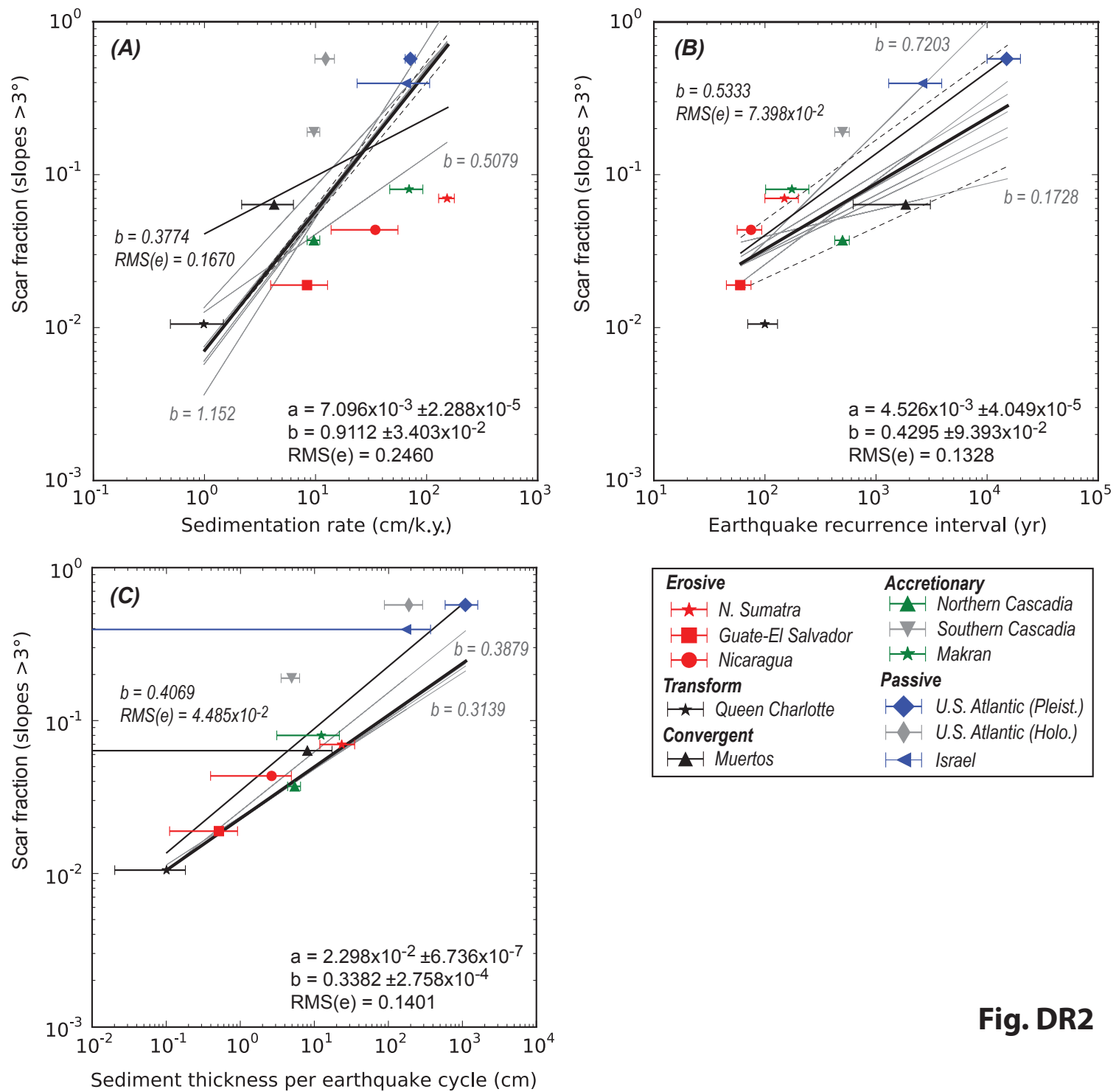


Fig. DR2